Graphene Quantum Dots/L-Cysteine Coreactant Electrochemiluminescence System and Its Application in Sensing Lead(II) Ions

Yongqiang Dong, Wanrong Tian, Shuyan Ren, Ruiping Dai, Yuwu Chi,* and Guonan Chen

Ministry of Education Key Laboratory of Analysis and Detection Technology for Food Safety, Fujian Provincial Key Laboratory of Analysis and Detection Technology for Food Safety, and Department of Chemistry, Fuzhou University, Fujian 350108, China

Ⓢ Supporting Information

ABSTRACT: A new coreactant electrochemiluminescence (ECL) system including single-layer graphene quantum dots (GQDs) and L-cysteine (L-Cys) was found to be able to produce strong cathodic ECL signal. The ECL signal of GQD/L-Cys coreactant system was revealed to be mainly dependent on some key factors, including the oxidation of L-Cys, the presence of dissolved oxygen and the reduction of GQDs. Then, a possible ECL mechanism was proposed for the coreactant ECL system. Furthermore, the ECL signal of the GQD/L-Cys system was observed to be quenched by lead(II) ions (Pb^{2+}). After optimization of some important experimental conditions, including concentrations of GQDs and L-Cys, potential scan rate, response time, and pH value, an ECL sensor was developed for the detection of Pb^{2+}. The new methodology can offer a rapid, reliable, and selective detection of Pb^{2+} with a detection limit of 70 nM and a dynamic range from 100 nM to 10 μM.

KEYWORDS: graphene quantum dots, L-cysteine, coreactant, electrochemiluminescence, lead(II)
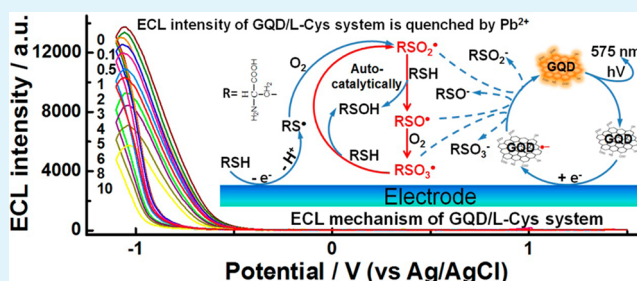
■ INTRODUCTION

Electrochemiluminescence (ECL) is a kind of luminescence produced during electrochemical reactions in solutions.[1] As an analytical technique, ECL combines advantages of chemiluminescent analysis (absence of background optical signal) with that of electrochemical analysis (ease of reaction control by applying electrode potential), and accordingly presents outstanding advantages including high sensitivity, selectivity, and wide response range.[2,3] Broad attention has been paid to the work of ECL, including the foundation studies and the analytical applications. As traditional ECL systems based on classic ECL luminophores (such as $Ru(bpy)_3^{2+}$ and its derivatives, and luminol) have been well-studied, more and more attention has been focused on developing new ECL systems based on new luminescent materials. In the past decade, many kinds of semiconductor-based quantum dots (QDs) have been found to have ECL activity,[4−6] and a series of analytical applications have been developed based on the ECL behaviors of those QDs.[7−9] However, further applications of these semiconductor-based QDs, especially the most studied cadmium-containing QDs, are usually limited by their poor stability and biocompatibility, and environmental toxicity.[10]

Carbon-based dots (CDs), emerging luminescent nanomaterials, usually include carbon nanoparticles of less than 10 nm in diameter (so-called carbon quantum dots, CQDs) and graphene nanosheets of usually less than 100 nm in lateral size (so-called graphene quantum dots, GQDs).[11,12] Like traditional

QDs, CDs exhibit unique electro-optical properties, and accordingly have attracted broad attention.[13−17] Recently, CDs were also found to be ECL active.[18] As ECL luminophores, CDs exhibit excellent ECL properties like those of other QDs. Furthermore, CDs present many obvious advantages over traditional QDs, such as excellent chemical inertness, easy labeling and nearly no toxicity.[13−15] Accordingly, CDs become promising alternatives of traditional QDs as ECL luminophores. However, not really much attention has been paid to the ECL study of CDs till now. In particular, the existing ECL studies about CDs were mainly focused on the CQDs.[18−21] Little attention has been paid to the ECL study of GQDs.[22] It has been reported that the ECL properties of CDs should be mainly dependent on their surface states.[18] Usually, GQD nanosheets, especially the single-layer GQDs, have higher specific surface areas than CQD nanoparticles, implying that GQDs might have more abundant surface states. Therefore, GQDs would have more potential than CQDs as ECL luminophores. Therefore, studying the ECL properties of GQDs is of significance. On the other hand, few coreactants (actually only peroxydisulfate and sulfite) have been found to increase the ECL signal of CDs, limiting seriously the ECL applications of CDs. Therefore, searching new compounds as

coreactants of the ECL reactions of CDs is very important. In the present study, we found that L-cysteine (L-Cys) could serve as a new coreactant of ECL reactions of single-layer GQDs. After investigating effects of some important conditions on the ECL response of GQD/L-Cys system, we proposed a possible ECL mechanism for the GQD/L-Cys system. Furthermore, we have applied the newly developed CD/L-Cys coreactant ECL system in the selective and sensitive detection of lead(II) ions (Pb^{2+}).

EXPERIMENTAL SECTION

Materials. Vulcan XC-72 carbon black was purchased from Cabot Corporation. $K_2S_2O_8$ (>99.99%) and L-cysteine (>99.5%) were obtained from Sigma-Aldrich. Lead(II) nitrate (>99.99%) was provided by Sinopharm Chemical Reagent Co, Ltd.. All other reagents were of analytical grade and used as received. Doubly distilled water was used throughout the experiments. 0.1 M phosphate buffer solutions (PBS) containing 1 M KNO_3 of different pH value were used for the ECL investigation.

Preparation of GQD Nanomaterials. GQDs were synthesized by chemical oxidization of XC-72 carbon black as described elsewhere.[23] Briefly, 1 g carbon black was refluxed with 250 mL 6 M HNO_3 at 130 °C for 24 h. Then heating was stopped and the suspension was cooled to room temperature. The suspension was centrifuged for 10 min to obtain an orange supernatant. The resultant supernatant was heated at 200 °C to remove the water and nitric acid. Finally, a reddish-brown solid was obtained.

Methods. One microliter of an aqueous suspension of GODs was drop-cast on freshly cleaved mica surface and dried in air. The samples were imaged in air by tapping-mode on a Nanoscope IIIa (Digital Instruments) with NSC15 tips (silicon cantilever, MikroMasch). UV−vis absorption spectra were characterized by a UV/vis/NIR spectrophotometer (Lambda 750). ECL and electrochemical measurements were carried out on an ECL detection system (MPI-E, Remex Electroic Instrument Ltd. Co., Xi'an, China) equipped with a homemade ECL cell mentioned elsewhere.[20] An atomic absorption (AAS) spectrophotometer (TAS-986, Beijing Persee Corporation, China) was used to detected the Pb^{2+} concentration of the Min River water sample.

Analysis of Real Sample. The water sample collected from Min River (Fujian, China) was filtered through a 0.22 μm membrane (Millipore) before measurement. Aliquots (500 μL) of the filtered water sample and spiked solutions were diluted to 1000 μL with PBS (0.2 M, pH 5) containing GQDs and L-Cys (the final concentrations of GQDs and L-Cys were 0.15 mg/mL and 0.5 mM, respectively) and then analyzed using the developed ECL sensor.

RESULTS AND DISCUSSION

The obtained GQDs are monodisperse nanosheets of ∼0.5 nm in average height (see Figure S1 in the Supporting Information). The emission wavelength of the GQDs is excitation-dependent, and is red-shift from 520 to 590 nm when the excitation wavelength is increased from 420 to 560 nm (see Figure S2 in the Supporting Information). All the results agree well with those of "single-layer graphene quantum dots" reported elsewhere,[23] suggesting that the GQDs used here should be single-layer graphene nanosheets with an average width of about 10 nm.

ECL Response and Mechanism of the GQD/L-Cys System. As shown in Figure 1, when the potential is cycled (scanned positively from 0 V) in the range from −1.10 to +1.50 V, GQDs or L-Cys alone produce only very weak cathodic ECL signals compared with the background of PBS. However, GQDs and L-Cys together produce a strong cathodic ECL signal. Furthermore, the strong cathodic ECL signal is very stable when the potential is cycled continuously between −1.10
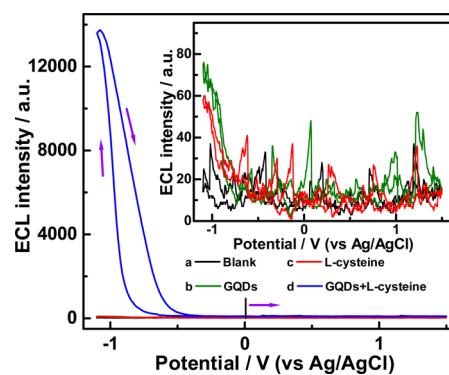

Figure 1. ECL potential curves of (a) PBS blank, (b) GQDs, (c) L-Cys, and (d) GQDs + L-Cys in air-saturated PBS (concentration of GQD, 0.15 mg/mL; concentration of L-Cys, 0.5 mM; pH 5; potential window, −1.10 to +1.50 V; scan rate, 0.6 V/s; onset potential, 0 V; scan direction, positive). Inset: amplification of lines a, b, and c.

and +1.50 V (see Figure S3 in the Supporting Information). The maximum emission wavelength of the ECL spectra was measured to be about 575 nm (see Figure S4 in the Supporting Information), which corresponds to the emission of the excited-sate CDs.[20] All the results imply that GQDs and L-Cys can form an excellent coreactant ECL system (GQD/L-Cys), in which GQDs are the luminophores while L-Cys acts as the coreactant.

The ECL response of GQD/L-Cys system is seriously dependent on the potential window. On the one hand, the ECL signal of the coreactant system can be observed only in the potential region of less than −0.75 V, and is the strongest at around −1.05 V (see Figure 1). Experimental results indicate that −0.75 V corresponds to the onset potential of the reduction of GQDs, whereas −1.05 V is near the potential where GQDs can be reduced most efficiently. (The effect of negative potential on the reduction efficiency of GQDs was measured using the method mentioned elsewhere,[20] and the experimental results are shown in Figure S5 in the Supporting Information.) As has been discussed in our previous study, the reduction of CDs is necessary for CD-based ECL systems to produce cathodic ECL signals.[18−20] Herein, the lower limit of potential window should mainly affect the reduction efficiency of GQDs, and then affect the ECL intensity of GQD/L-Cys system. On the other hand, the upper limit of potential window is also very important for the ECL response of GQD/L-Cys system. The cathodic ECL can be produced only when the upper limit of potential is more positive than +0.80 V. As the upper limit of potential window is increased gradually from +0.80 to +1.80 V while the lower limit of potential window is kept at −1.10 V, the ECL intensity of the GQD/L-Cys system increases gradually and reaches a maximum at +1.50 V, and then decreases (see Figure S6 in the Supporting Information). Figure 2 shows the cyclic voltammograms (CVs). Compared with the blank (curve a), GQDs produce nearly no obvious electrochemical response (curve b), whereas L-Cys gives a large irreversible oxidation current (curve c). Therefore, a preoxidation of L-Cys should be necessary for the ECL reactions of the GQD/L-Cys system. However, when L-Cys is well-oxidized at +1.50 V using a constant potential mode, the final oxidation products are not able to increase the cathodic ECL signal of GQDs. On the basis of the results discussed above, there should be some unstable intermediates (most likely free
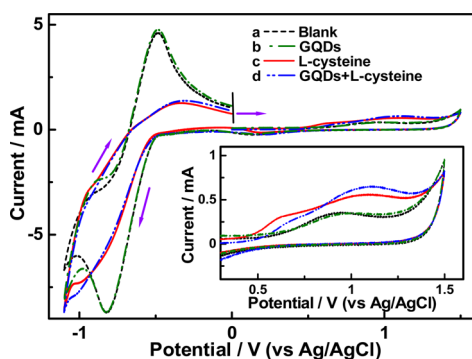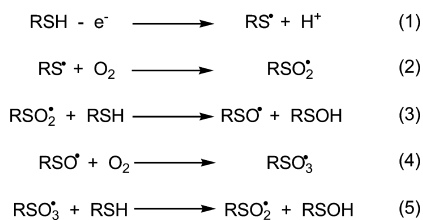
1647

dx.doi.org/10.1021/am404552s | ACS Appl. Mater. Interfaces 2014, 6, 1646−1651

Figure 2. Cyclic voltammogram of (a) PBS blank (b), GQDs, (c) L-Cys, and (d) GQDs + L-Cys in air-saturated PBS (concentration of GQD, 0.15 mg/mL; concentration of L-Cys, 0.5 mM; pH 5; potential window, −1.10 to +1.50 V; scan rate, 0.6 V/s; initial potential, 0 V; scan direction, positive). Inset, amplification of the four lines in the potential range of 0.3 to 1.5 V.

radicals) produced during the oxidation of L-Cys involved in the cathodic ECL reactions.

The oxidation of L-Cys is a complex procedure, in which abundant free radical intermediates may be produced.[24−26] As shown in Scheme 1, the thiol group of L-Cys (RSH) is readily

Scheme 1. Electrochemical Oxidation Mechanism of Thiol Group in the Presence of O_2

$$RSH - e^- \longrightarrow RS^{\bullet} + H^+ \quad (1)$$

$$RS^{\bullet} + O_2 \longrightarrow RSO_2^{\bullet} \quad (2)$$

$$RSO_2^{\bullet} + RSH \longrightarrow RSO^{\bullet} + RSOH \quad (3)$$

$$RSO^{\bullet} + O_2 \longrightarrow RSO_3^{\bullet} \quad (4)$$

$$RSO_3^{\bullet} + RSH \longrightarrow RSO_2^{\bullet} + RSOH \quad (5)$$

electrochemically oxidized into $RS^{\bullet}$ radical (reaction 1), which is further oxidized by dissolved oxygen molecules (O_2) to $RSO_2^{\bullet}$ radical (reaction 2). The produced $RSO_2^{\bullet}$ radical subsequently involves in a possible three-step autocatalytic reaction: 1) $RSO_2^{\bullet}$ reacts with RSH to form RSOH and $RSO^{\bullet}$ (reaction 3); 2) $RSO^{\bullet}$ is further oxidized to $RSO_3^{\bullet}$ by the dissolved O_2 (reaction 4); 3) $RSO_3^{\bullet}$ is reduced by RSH to produce RSOH and $RSO_2^{\bullet}$ (reaction 5). Therefore, the oxidation of L-Cys during the anodic polarization process produces at least four kinds of free radicals, including $RS^{\bullet}$, $RSO^{\bullet}$, $RSO_2^{\bullet}$, and $RSO_3^{\bullet}$. Generally speaking, these free radicals are very unstable. It seems unreasonable that these free radicals are still present during the following cathodic polarization process. However, except for $RS^{\bullet}$, the other three kinds of free radicals are produced all the time because of the autocatalytic reactions (reactions 2−5), and might participate in the cathodic ECL reactions. Apparently, O_2 should be an important factor to the formation of these free radicals. The effect of O_2 on the ECL response of GQD/L-Cys system was accordingly investigated using the same method mentioned in our previous work.[20] Experimental results indicate that the GQD/L-Cys system produces a very weak ECL signal in the absence of O_2 whereas gives rise to a strong ECL signal in the presence of O_2 (see Figure S7 in the Supporting Information), further confirming that the three kinds of free radicals ($RSO^{\bullet}$, $RSO_2^{\bullet}$, and $RSO_3^{\bullet}$) should be related to the cathodic ECL reactions.

Based on the discussion above, the thiol group should be the key factor of the ECL reactions. To further confirm the role of the thiol group, another thiol group-containing compound, i.e., thioglycollic acid (without ECL activity itself), was used as the coreactant instead of L-Cys. Similar ECL behaviors were observed (see Figure S8 in the Supporting Information). Herein, a reasonable ECL mechanism can be proposed for the GQD/L-Cys system. As shown in Figure 3, on the one hand,
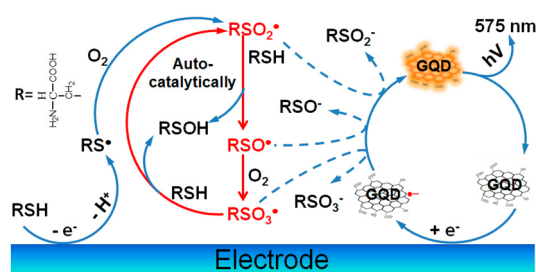

Figure 3. Diagram for the ECL reaction mechanism of the GQD/L-Cys system.

the thiol group of L-Cys is electro-oxidized in the anodic polarization process to produce $RS^{\bullet}$, which is further oxidized to $RSO_2^{\bullet}$ by O_2 dissolved in the solution. Subsequently, the formed $RSO_2^{\bullet}$ initiates a three-step autocatalytic reaction, in which three kinds of free radicals ($RSO^{\bullet}$, $RSO_2^{\bullet}$, and $RSO_3^{\bullet}$) are produced continuously. On the other hand, GQDs are electro-reduced in the following cathodic polarization process to produce negatively charged GQDs. Meanwhile, electron transfer occurs between the negatively charged GQDs and the three kinds of free radicals, producing excited-state GQDs. Finally, ECL signal is produced when the excited-state GQDs go back to their ground states.

Establishment of the ECL Sensing Method for Pb^{2+}. On the basis of the strong ECL signal, the developed GQD/L-Cys system was applied in the detection of Pb^{2+}, a well-known environmental pollutant. Pb^{2+} is quite harmful to human being. It may cause serious damage to brain and central nervous system even at a very small dose.[27,28] Therefore, the development of sensors to detect Pb^{2+} is of great importance. Accordingly, we tried to develop a new ECL sensor for Pb^{2+} based on GQD/L-Cys system.

Some experimental conditions affecting the ECL intensity were first optimized prior to the detection of Pb^{2+}. Apparently, the ECL intensity of GQD/L-Cys system is affected by the concentration of the luminophore. As shown in Figure 4a, ECL intensity increases sharply with the concentration of GQDs in the range of 0 to 0.15 mg/mL, but tends to be stable when the concentration of GQDs is further increased. Accordingly, 0.15 mg/mL GQDs was used in the sensing system. As a coreactant ECL system, the ECL intensity of GQD/L-Cys system is also affected by the concentration of L-Cys. As shown in Figure 4b, the ECL intensity increases linearly with the concentration of L-Cys in the range of 0.05 to 0.5 mM, but increases slightly when the concentration of L-Cys is further increased. For obtaining high sensitivity while decreasing reagent consumption, 0.5 mM was adopted as the concentration of L-Cys in the sensing system. The ECL intensity of GQD/L-Cys system can also be affected by the potential scan rate. As shown in Figure 4c, the ECL intensity increases obviously with the scan rate in the range of 0.05−0.6 V/s, and tends to be stable when the scan
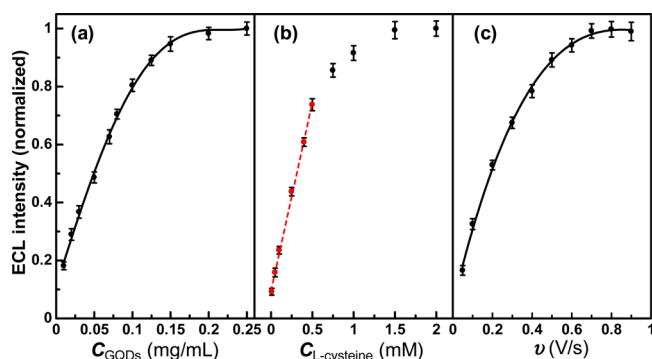
Figure 4. (a) Effect of GQD concentration on the ECL intensity of GQD/L-Cys system (concentration of L-Cys, 0.5 mM; scan rate, 0.6 V/s; pH 5). (b) Effect of L-Cys concentration on the ECL intensity of GQD/L-Cys system (concentration of GQD, 0.15 mg/mL; scan rate, 0.6 V/s; pH 5). (c) Effect of scan rate on the ECL intensity of GQD/L-Cys system (concentration of GQD, 0.15 mg/mL; concentration of L-Cys, 0.5 mM; pH 5).

rate is higher than 0.6 V/s. Therefore, the ECL sensing system for Pb^{2+} was carried out at the potential scan rate of 0.6 V/s.

The response rate of the ECL signal of the GQD/L-Cys system to Pb^{2+} was then investigated. The ECL intensity is quenched by 60% as soon as 10 μM Pb^{2+} is added into the GQD/L-Cys system, and remains stable in the following 1 h observation (see Figure S9 in the Supporting Information). Apparently, the quenching effect of Pb^{2+} on the ECL signal of the GQD/L-Cys system is quite rapid and stable, implying a promising application in a fast sensing of Pb^{2+} without strict time control.

The pH value of solution was found to be an important factor for the sensing system. On the one hand, it affects obviously the ECL intensity of the GQD/L-Cys system. As shown in Figure 5 (black columns), the GQD/L-Cys system shows strong ECL in solutions of pH 5−7, but weak ECL in solutions of other pH values, especially in alkaline solutions. The pH dependence of the ECL intensity may be related to the stability of the free radicals (RSO$^\bullet$, RSO$_2$$^\bullet$, and RSO$_3$$^\bullet$) in different pH value. On the other hand, the pH value also affects
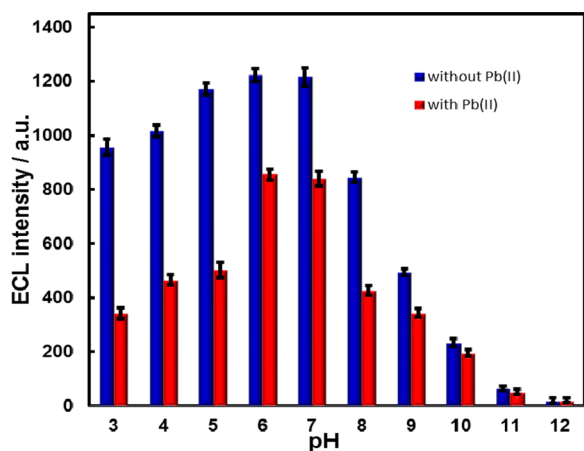

Figure 5. ECL response of the GQD/L-Cys system in the absence and presence of 10 μM Pb^{2+} in air-saturated PBS of serial pH values (concentration of GQD, 0.15 mg/mL; concentration of L-Cys, 0.5 mM; potential window, −1.10 to +1.50 V; scan rate, 0.6 V/s; onset potentia, 0 V; scan direction, positive).

the quenching efficiency of Pb^{2+} on the ECL intensity of GQD/L-Cys system (($I_0 - I$)/I_0, where I_0 and I are ECL intensities of the GQD/L-Cys system in the absence and presence of Pb^{2+}, respectively). As shown in Figure 5 (red columns), the quenching efficiency is relative high in solutions of pH ≤5, whereas it is much lower in solutions of pH >5. Furthermore, the quenching efficiency decreases with the increase of pH value, which may be related to the hydrolysis of Pb^{2+}. Accordingly, pH 5 was chosen for the sensing system.

Sensitivity of the Sensing System. Under the optimum conditions discussed above, the linear response range of the sensing system was measured. As shown in Figure 6, the ECL
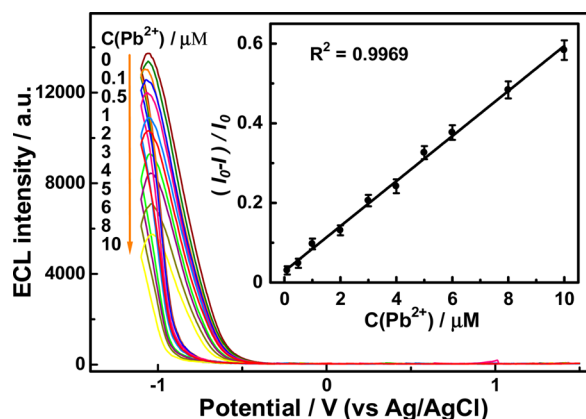

Figure 6. ECL response of GQD/L-Cys system upon addition of serial concentrations of Pb^{2+} in air-saturated PBS (from top: 0, 0.1, 0.5, 1, 2, 3, 4, 5, 6, 8, 10 μM) (concentration of GQD, 0.15 mg/mL; concentration of L-Cys, 0.5 mM; potential window, −1.10 to +1.50 V; scan rate, 0.6 V/s; onset potential, 0 V; scan direction, positive; pH 5). Inset: Linear calibration plot for Pb^{2+} detection.

intensity of GQD/L-Cys system is sensitive to Pb^{2+}, and decreases obviously with the increase of the concentration of Pb^{2+}. A good linear relationship between the quenching ratio and the concentration of Pb^{2+} has been observed in the range from 0.10 to 10 μM (see inset of Figure 6 and eq 6):

$$(I_0 - I)/I_0 = 5.660 \times 10^4 C + 0.028 \ (R^2 = 0.997) \quad (6)$$

where C is the concentration of Pb^{2+}. In this case, the detection limit of Pb^{2+} was calculated to be 70 nM. Although the detection limit of this sensor is not as good as those of some DNAzyme-based sensors,[29−31] it is comparable with those of some methods based on other nanoparticles.[32−35] Furthermore, this sensor shows many advantages such as low-cost, simple, and fast operation, and environmental friendliness. Accordingly, the ECL sensor would have great potential in biological and environmental applications.

Specificity of the Sensing System. Selectivity is another important issue to assess the performance of a new proposed sensor, and should be accordingly evaluated. Besides Pb^{2+}, several commonly existing metal ions including Hg^{2+}, Cu^{2+}, Co^{2+}, Fe^{3+}, Ni^{2+}, Ag$^+$, Ca^{2+}, Cd^{2+}, Mn^{2+}, Mg^{2+}, Ba^{2+}, Na$^+$, Li$^+$, Cr$_2$O$_7$$^{2-}$, and Zn^{2+} were investigated. The counteranions were NO$_3$$^-$ or Cl$^-$, which were also proved to have no obvious effect on the ECL of GQD/L-Cys system. As shown in Figure 7, only Pb^{2+} quenches dramatically the ECL intensity of GQD/L-Cys system, whereas other ions quench the ECL intensity very slightly (e.g., Hg^{2+}, Cu^{2+}, Co^{2+}, Fe^{3+}, Ni^{2+}, and Ag$^+$) or have nearly no effect (Ca^{2+}, Cd^{2+}, Mn^{2+}, Mg^{2+}, Ba^{2+}, Na$^+$, Li$^+$,
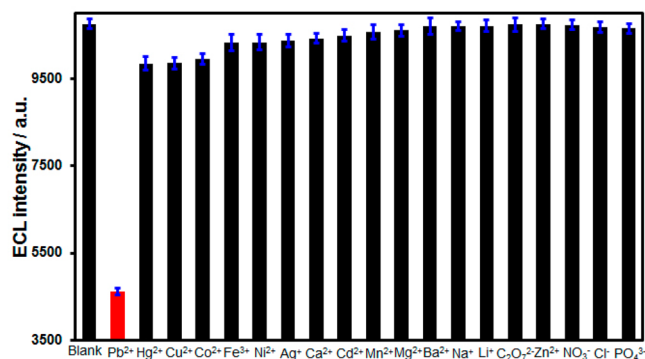
Figure 7. Selectivity of the GQD/L-Cys system based sensor for Pb^{2+} over other ions in air-saturated PBS (concentration of GQD, 0.15 mg/mL; concentration of L-Cys, 0.5 mM; potential window, −1.10 to +1.50 V, scan rate, 0.6 V/s; onset potential, 0 V; scan direction, positive; pH 5; concentrations of all metal ions and anions are 10 μM).

$Cr_2O_7^{2-}$, and Zn^{2+}) on the ECL intensity. This result indicates that the sensing system has high specificity toward Pb^{2+}. We have confirmed the high specificity of the GQD/L-Cys ECL toward Pb^{2+} by experiments for many times; however, we have not obtained adequate explanation for this result yet. Probably, it might result from specific catalysis of Pb^{2+} ions toward the oxidation of L-Cys, which will be further discussed in the ECL quenching mechanism below.

Mechanism of the ECL Quenching of GQD/L-Cys System by Pb^{2+}. As mentioned above, the ECL signal of GQD/L-Cys system can be selectively and sensitively quenched by Pb^{2+}. It is worth discussing the quenching mechanism. The ECL quenching may be through either quenching the exited-state GQDs directly or blocking the formation of exited-state GQDs. In a control experiment, Pb^{2+} had nearly no quenching effect on the ECL responses of the $GQD/S_2O_8^{2-}$ system in the potential range of 0 to −1.10 V, no matter whether L-Cys was used or not (see Figure S10 in the Supporting Information). This result suggests that Pb^{2+} or its complexes with L-Cys is not able to quench the exited-state GQDs. In other words, Pb^{2+} may block the formation pathway of excited-state GQDs. As has been discussed above, the formation of the excited-state GQDs involves the productions of negatively charged GQDs and three kinds of free radicals ($RSO^{\bullet}$, $RSO_2^{\bullet}$, and $RSO_3^{\bullet}$). The fact that Pb^{2+} does not quench the ECL of $GQD/S_2O_8^{2-}$ system (involving the productions of negatively charged GQDs and $SO_4^{\bullet-}$) also implies that Pb^{2+} has no obvious effect on the formation or stability of the negatively charged GQDs. Therefore, The ECL quenching of GQD/L-Cys system by Pb^{2+} is most likely through inhibiting the formation of the three kinds of free radicals ($RSO^{\bullet}$, $RSO_2^{\bullet}$, and $RSO_3^{\bullet}$) from the oxidation of L-Cys. This conclusion can be further supported by previous reports that some heavy metal ions would affect (either catalyze or quench) the oxidation of thiol group.[24,36−38]

Application. The practical application of the sensing system was demonstrated in the determination of Pb^{2+} in river water sample collected from Min River (the largest river in Fujian Province, China). Experimental results showed that the river water had no observable effect on the ECL intensity of GQD/L-Cys system, indicated Pb^{2+} in the water sample was not detected (below the lowest detectable concentration of the method). The river water sample was also proved to have no detectable Pb^{2+} using an AAS method. Thus then the water sample was spiked with 6 μM Pb^{2+}, and tested with the sensing

system. The recovery was calculated to be 102%, implying that the developed sensor could be applicable to real water samples.

CONCLUSIONS

In summary, a new GQD/L-Cys coreactant ECL system has been developed. In the anodic polarization process, the thiol group of L-Cys is first oxidized into $RS^{\bullet}$ radical, which soon reacts with the dissolved O_2 to form $RSO_2^{\bullet}$ radical. Subsequently, a three-step autocatalytical reaction is initiated, producing abundant free radical intermediates ($RSO^{\bullet}$, $RSO_2^{\bullet}$, and $RSO_3^{\bullet}$) near the surface of the working electrode all the time. In the following cathodic polarization process, those free radicals reacted with the electro-reduced GQDs to form excited-state GQDs. Subsequently, a strong cathodic ECL signal is produced. Furthermore, based on the ECL of the GQD/L-Cys system, a sensor for the detection of Pb^{2+} has been developed. The Pb^{2+} sensor shows many advantages including rapid detection, good selectively, high sensitivity, and low cost. The present work not only might enrich the foundation study about the ECL properties of GQDs but also would promote the analytical application of GQDs.

ASSOCIATED CONTENT

ⓢ Supporting Information

AFM image of GQDs (Figure S1), fluorescence spectra of GQDs (Figure S2), ECL response and ECL spectrum of the GQD/L-Cys system (Figures S3 and S4), effect of negative potential on the reduction efficiency of GQDs (Figure S5), effects of upper limit of potential window and dissolved oxygen concentration on the ECL intensity of the GQD/L-Cys system (Figures S6 and S7), CV and ECL response of the GQD/thioglycollic acid system (Figure S8), response time of the GQD/L-Cys system to Pb^{2+} (Figure S9), and ECL response of the $GQD/S_2O_8^{2-}$ system to Pb^{2+} (Figure S10). This material is available free of charge via the Internet at http://pubs.acs.org.

AUTHOR INFORMATION

Corresponding Author
*E-mail: y.w.chi@fzu.edu.cn. Fax/Tel: +86-591-22866137.

Notes
The authors declare no competing financial interest.

ACKNOWLEDGMENTS

REFERENCES

(1) Miao, W. *Chem. Rev.* **2008**, *108*, 2506−2553.
(2) Yin, X. B.; Dong, S.; Wang, E. *TrAC, Trends Anal. Chem.* **2004**, *23*, 432−441.
(3) Gerardi, R. D.; Barnett, N. W.; Lewis, S. W. *Anal. Chim. Acta* **1999**, *378*, 1−41.
(4) Ding, Z.; Quinn, B. M.; Haram, S. K.; Pell, L. E.; Korgel, B. A.; Bard, A. J. *Science* **2002**, *296*, 1293−1297.
(5) Myung, N.; Ding, Z.; Bard, A. J. *Nano Lett.* **2002**, *2*, 1315−1319.
(6) Bae, Y.; Myung, N.; Bard, A. J. *Nano Lett.* **2004**, *4*, 1153−1161.
(7) Zou, G.; Ju, H. *Anal. Chem.* **2004**, *76*, 6871−6876.
(8) Jiang, H.; Ju, H. *Anal. Chem.* **2007**, *79*, 6690−6696.
(9) Shan, Y.; Xu, J.; Chen, H. *Chem. Commun.* **2009**, *8*, 905−907.

(10) Michalet, X.; Pinaud, F. F.; Bentolila, L. A.; Tsay, J. M.; Doose, S.; Li, J. J.; Sundaresan, G.; Wu, A. M.; Gambhir, S. S.; Weiss, S. *Science* **2005**, *307*, 538−544.

(11) Sun, Y. P.; Zhou, B.; Lin, Y.; Wang, W.; Fernando, K. A. S.; Pathak, P.; Meziani, M. J.; Harruff, B. A.; Wang, X.; Wang, H. F.; Luo, P. J. G.; Yang, H.; Kose, M. E.; Chen, B. L.; Veca, L. M.; Xie, S. Y. *J. Am. Chem. Soc.* **2006**, *128*, 7756−7757.

(12) Ponomarenko, L. A.; Schedin, F.; Katsnelson, M. I.; Yang, R.; Hill, E. W.; Novoselov, K. S.; Geim, A. K. *Science* **2008**, *320*, 356−358.

(13) Baker, S. N.; Baker, G. A. *Angew. Chem., Int. Ed.* **2010**, *49*, 6726−6744.

(14) Zhang, Z.; Zhang, J.; Chen, N.; Qu, L. *Energy Environ. Sci.* **2012**, *5*, 8869−8890.

(15) Shen, J.; Zhu, Y.; Yang, X.; Li, C. *Chem. Commun.* **2012**, *48*, 3686−3699.

(16) Sun, H.; Gao, N.; Wu, L.; Ren, J.; Wei, W.; Qu, X. *Chem.—Eur. J.* **2013**, *19*, 13362−13368.

(17) Zhou, L.; Lin, Y.; Huang, Z.; Ren, J.; Qu, X. *Chem. Commun.* **2012**, *48*, 1147−1149.

(18) Zheng, L.; Chi, Y.; Dong, Y.; Lin, J.; Wang, B. *J. Am. Chem. Soc.* **2009**, *131*, 4564−4565.

(19) Dong, Y.; Zhou, N.; Lin, X.; Lin, J.; Chi, Y.; Chen, G. *Chem. Mater.* **2010**, *22*, 5895−5899.

(20) Dong, Y.; Chen, C.; Lin, J.; Zhou, N.; Chi, Y.; Chen, G. *Carbon* **2013**, *56*, 12−17.

(21) Zhu, H.; Wang, X.; Li, Y.; Wang, Z.; Yang, F.; Yang, X. *Chem. Commun.* **2009**, 5118−5120.

(22) Li, L.; Li, J.; Fei, R.; Wang, C.; Lu, Q.; Zhang, J.; Jiang, L.; Zhu, J. *Adv. Funct. Mater.* **2012**, *22*, 2971−2979.

(23) Dong, Y.; Chen, Q.; Zheng, X.; Gao, L.; Cui, Z.; Yang, H.; Guo, C.; Chi, Y.; Li, C. *J. Mater. Chem.* **2012**, *22*, 8764−8766.

(24) Capozzi, G.; Modena, G. In *The Thiol Group*; Patai, S., Ed.; John Wiley & Sons: Chichester, U.K., 1974; Chapter 17, pp 785−839.

(25) Quijano, C.; Alvarez, B.; Gatti, R. M.; Augusto, O.; Radi, R. *Biochem. J.* **1997**, *322*, 167−173.

(26) Ho, S.; Chiu, S.; Hu, T. *Free Radical Res.* **2012**, *46*, 1190−1200.

(27) Godwin, H. A. *Curr. Opin. Chem. Biol.* **2001**, *5*, 223−227.

(28) Needleman, H. *Annu. Rev. Med.* **2004**, *55*, 209−222.

(29) Lan, T.; Furuya, K.; Lu, Y. *Chem. Commun.* **2010**, *46*, 3896−3898.

(30) Liu, J. W.; Lu, Y. *Anal. Chem.* **2003**, *75*, 6666−6672.

(31) Xiang, Y.; Tong, A.; Lu, Y. *J. Am. Chem. Soc.* **2009**, *131*, 15352−15357.

(32) Fu, X.; Lou, T.; Chen, Z.; Lin, M.; Feng, W.; Chen, L. *ACS Appl. Mater. Interfaces* **2012**, *4*, 1080−1086.

(33) Yoosaf, K.; Ipe, B. I.; Suresh, C. H.; Thomas, K. G. *J. Phys. Chem. C* **2007**, *111*, 12839−12847.

(34) li, E. M.; Zheng, Y.; Yu, H.; Ying, J. Y. *Anal. Chem.* **2007**, *79*, 9452−9458.

(35) Chai, F.; Wang, C.; Wang, T.; Li, L.; Su, Z. *ACS Appl. Mater. Interfaces* **2010**, *2*, 1466−1470.

(36) Munday, R.; Munday, C. M.; Winterbourn, C. C. *Free Radical Biol. Med.* **2004**, *36*, 757−764.

(37) Seanor, D. A.; Swift, J. A. *Polymer* **1978**, *19*, 934−938.

(38) Jakob, U.; Reichmann, D. In *Oxidative Stress and Redox Regulation*; Conte, M. L.; Carroll, K. S., Eds.; Springer: Dordrecht, The Netherlands, 2013; Chapter 1, pp 1−42.